Wheat Yield Functions for Analysis of Land-Use Change in China

Cynthia Rosenzweig
NASA, Goddard Institute for Space Studies, New York, NY, USA

Ana Iglesias
Polytechnical University of Madrid, Spain

Günther Fischer
International Institute for Applied Systems Analysis, Laxenburg, Austria

Yanhua Liu
The State Commission of Science and Technology, Beijing, China

Walter Baethgen
International Fertilizer Development Center, Montevideo, Uruguay

James W. Jones
University of Florida, Gainesville, FL, USA

RR-00-15
June 2000

Reprinted from *Environmental Modeling and Assessment 4 (1999) 115–132.*

International Institute for Applied Systems Analysis • Schlossplatz 1 • A-2361 Laxenburg • Austria
Tel: (+43 2236) 807 • Fax: (+43 2236) 71313 • E-mail: publications@iiasa.ac.at • Web: www.iiasa.ac.at

Reprinted with permission from *Environmental Modeling and Assessment* 4 (1999) 115–132.

Wheat yield functions for analysis of land-use change in China

Cynthia Rosenzweig, Ana Iglesias, Günther Fischer, Yuanhua Liu, Walter Baethgen and James W. Jones

Received 28 July 1998; revised 3 February 1999

CERES-Wheat, a dynamic process crop growth model, is specified and validated for eight sites in the major wheat-growing regions of China. Crop model results are then used to test the Mitscherlich–Baule and the quadratic functional forms for yield response to nitrogen fertilizer, irrigation water, temperature, and precipitation. The resulting functions are designed to be used in a linked biophysical–economic model of land-use and land-cover change in China. While both functions predict yield responses adequately, the Mitscherlich–Baule function is preferable to the quadratic function because its parameters are biologically and physically realistic. Variables explaining a significant proportion of simulated yield variance are nitrogen, irrigation water, and precipitation; temperature was a less significant component of yield variation within the range of observed year-to-year variability at the study sites. Crop model simulations with a generic soil with median characteristics of the eight sites compared to simulations with site-specific soils showed that agricultural soils in China have similar and, in general, low-to-moderate water-holding capacities and organic matter contents. The validated crop model is useful for simulating the range of conditions under which wheat is grown in China, and provides the means to estimate production functions when experimental field data are not available.

Keywords: agriculture, land use, wheat production, simulation models, China

1. Introduction

China is undergoing rapid changes in economic structure and development, urban and rural lifestyles, demands on land and water resources, and pressures on the environment. Its population is predicted to continue to grow for at least another 30 years, and to reach a population level of about 1.4–1.5 billion people by the year 2030 [5]. Recognizing the need to project potential courses of agricultural development, the International Institute for Applied Systems Analysis (IIASA) Land-Use and Land-Cover Change (LUC) Project is assembling a set of databases and analytical tools relating to China [4,11]. These tools combine biophysical understanding of agro-ecosystem processes [22] and a compilation of land and water resources into a linked biophysical–economic model of land-use and land-cover change.

The IIASA LUC China model combines welfare analysis and the general equilibrium approach with a spatially explicit representation of land productivity and actor-based decisions [4]. The economic model maximizes intertemporal social welfare at the national level with disaggregation into eight regions. Crop production functions are needed to represent revenue-maximizing decisions by the farmer at the regional level; such decisions, in turn, lead to projections of regional land-use change in the model [13].

Wheat is the third major grain crop in China, after rice and maize. It is currently grown in many regions with productivity levels that depend greatly on management inputs. In 1998, China produced about 110 million tons of wheat [6]. Here we utilize a calibrated and validated dynamic process crop growth model, CERES-Wheat [20], and data from the IIASA-LUC Geographic Information System (GIS) to test site-based crop responses to management, specifically nitrogen fertilizer and water for irrigation, for the observed range of interannual climate variability (see references for China data).

Thompson [25], Baier [2], Ramirez et al. [16], and Waggoner [26] are among those who have developed regression equations from observed data, finding that precipitation, temperature, and nitrogen fertilizer, and derived variables such as soil moisture, growing degree days, and potential evapotranspiration were key factors in wheat yield prediction. Thompson [25] found that monthly precipitation and temperature in key growing season months and technology trends (primarily nitrogen fertilization) accounted for 80–92% of wheat yield variability in six important wheat-growing states in the U.S. between 1945 and 1968. Crop yield responses to inputs, such as fertilizer and water, have often been specified as polynomial functions such as the quadratic or square root forms.

Quadratic functions are relatively easy to estimate because they are linear in their parameters and exhibit diminishing marginal productivity and input substitution [15]. However, they have been shown to be unrealistic in that they force input substitution, do not allow for growth plateaus as do the von Liebig and Mitscherlich–Baule forms, and tend to overestimate the optimal fertilizer quantity [1,7]. Ackello-Ogutu et al. [1] found that the von Liebig function was preferred to the square root and quadratic forms in representing fertilizer responses of corn, soybean, wheat, and hay in Indiana, as did Grimm et al. [10].

Crop simulation models have been used to develop yield response functions to inputs where limited experimental data restrict further evaluation of functional forms [15].

Sheierling et al. [23] tested the impact of irrigation timing using simulated water-crop production functions developed with the van Genuchten–Hanks model.

Here we test two regression models utilizing simulated crop yield responses as possible yield functions for the IIASA model of land-use and land-cover change: the quadratic and the Mitscherlich–Baule (MB). The quadratic function tested imposes non-zero elasticity of substitution among factors and diminishing marginal productivity:

$$Y_i = \alpha_1 + \alpha_2(N_i) + \alpha_3(W_i) + \alpha_4(N_i)^2 + \alpha_5(W_i)^2 + \alpha_6(N_i W_i),$$

where Y_i is wheat yield (kg ha^{-1}), N_i is nitrogen applied (kg ha^{-1}), W_i is total water amount (precipitation plus irrigation) received by the crop (mm), the subscript i refers to year, and α_1–α_6 are parameters.

The Mitscherlich–Baule function has been found to be preferable for use in an economic model because it allows for factor substitution and a growth plateau following von Liebig's "Law of the Minimum" [15]. The use and usefulness of the MB function in the IIASA LUC model is discussed in [13]. The MB function is of the form

$$Y_i = \beta_1\left(1 - \exp\left(-\beta_2(\beta_3 + N_i)\right)\right) \times \left(1 - \exp\left(-\beta_4(\beta_5 + W_i)\right)\right),$$

where the variables are as described above, and β_1–β_5 are parameters. β_1 represents an asymptotic yield level plateau; β_3 and β_5 can be interpreted as the residual levels of nitrogen and water in the soil.

The objective of this study is to determine the variables that explain a significant proportion of simulated yield variance at sites spanning the major wheat-growing region of China and to specify appropriate functional forms for use in the IIASA-LUC model. The crop model is used because experimental agronomic data are lacking across the large area where wheat is grown in China. The crop models further provide testable results at sites for the more spatially generalized scale used in the land-use change model.

2. Methods

2.1. Sites

CERES-Wheat is calibrated and validated across eight sites spanning the wheat-growing regions of China (figure 1 and table 1). The sites represent the climate conditions under which wheat is grown in China, ranging from the continental climate of the traditional wheat-growing regions in the North China Plain (Beijing and Liaocheng) to the moderately warm subtropical zone in the center of the country (Chengdu). Yulin represents the marginal desert-transition zone of the loess plateau; Xi'an lies in the central reaches of the Yellow River basin; and Xuzhou, Suzhou and Nanjing are found in the fertile plain of the Yangtze River. Winter wheat is grown in the cooler areas; in the warmer areas, spring wheat is sown in the late fall and matures without vernalization. Both rainfed and irrigated wheat areas are represented, as specified by the IIASA-LUC county-level data (see references for China data).

2.2. Crop model

Yield responses to climate and management were simulated with CERES-Wheat [9,19,20], a process-based mechanistic model that simulates daily phenological development and growth in response to environmental factors (soil and climate) and management (crop variety, planting conditions, nitrogen fertilization, and irrigation). The model is designed to have applicability in diverse environments and to utilize a minimum data set of commonly available field and weather data as inputs. CERES-Wheat has been calibrated and validated over a wide range of agroclimatic regions [22].

In order to determine the aboveground crop response to water, CERES-Wheat calculates the soil water balance (infiltration and runoff, soil evaporation, crop transpiration, and drainage) [18]. Whenever crop extraction of soil water falls below the potential transpiration rate calculated for the crop, the resulting water stress reduces dry matter production rate below maximum, resulting in yield declines. Thus, the model may be used to evaluate yield reduction caused by soil and plant water deficits. Irrigation regimes may easily be tested through specification of timing and amount of water deliveries, or through the application of "automatic" irrigation water when soil moisture drops to a specified threshold level.

Temperature is an important variable in the CERES-Wheat model, because crop phenology (progression of the crop through its development stages) is calculated primarily through the accumulation of temperature above a base temperature (growing degree days). Duration of grain-filling, a key determinant of yield, thus depends in part on temperature. Dry matter production and number of grains per head are also temperature-dependent in the model.

The response of the wheat crop to nitrogen deficits is also calculated in CERES-Wheat [8]. The model calculates a critical N concentration in the plant tissue below which growth will be reduced. These concentrations are determined as a function of crop development stage and are used within the model to simulate the effects of N deficiency. Nitrogen dynamics in the model include mineralization and/or immobilization of N associated with the decay of crop residues, nitrification, denitrification, urea hydrolysis, leaching of nitrate, and the uptake and use of N by the crop. The N model uses the layered soil-water balance model described by Ritchie [18] and the soil temperature component of the EPIC model [27]. The nitrogen formulation in CERES-Wheat has been tested in diverse environments (see, e.g., [8,14,24]), and been found, in general, to provide reasonable predictions of N uptake by the aboveground plant and the partitioning of this N into grain.

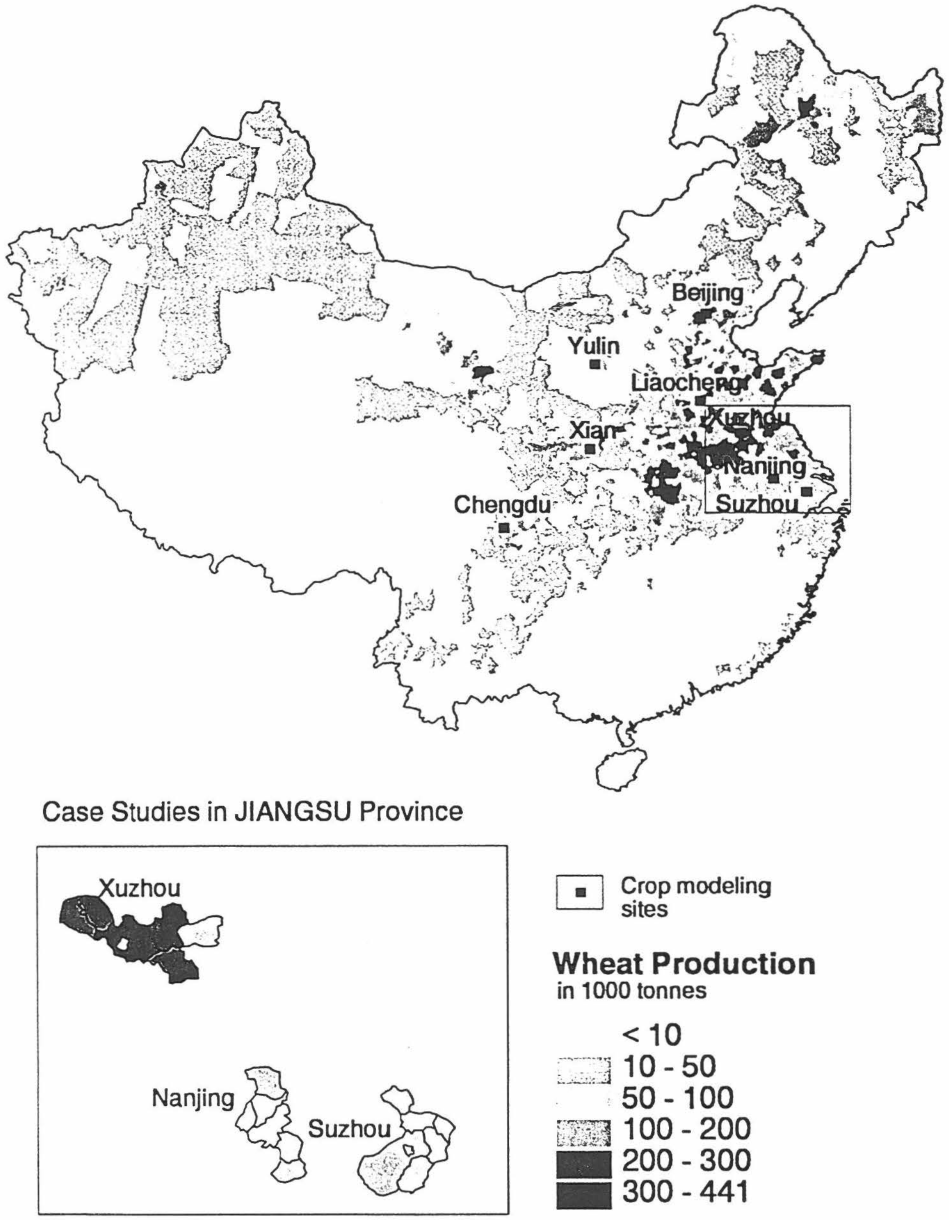

Figure 1. Wheat-growing areas and study sites in China.

2.3. Inputs

Climate. Daily climate variables (maximum and minimum temperature and precipitation) for the eight sites were provided by Dr. Roy Jenne of the U.S. National Center for Atmospheric Research. Time-series for the different sites ranged from 15 to 30 years. Daily solar radiation for each time-series was generated using the WGEN weather generator [17].

Figure 2 shows average monthly temperature and precipitation for the sites and table 1 shows the length of record, the average annual temperature and precipitation, and the

Table 1
Site, province, latitude and longitude, length of daily climate record, mean annual temperature and precipitation, and mean wheat growing-period precipitation at crop-modeling sites.

Site	Province	Lat.[a]	Long.[a]	Years[b]	Temp. (SD) (°C)	Prec. (SD) (mm)	GP[c] prec. (SD) (mm)
Beijing	Beijing	39.97	116.32	58–77	12.6 (0.6)	636 (258)	152 (84)
Liaocheng	Shandong	36.02	115.35	79–95	14.1 (0.3)	482 (126)	178 (68)
Yulin	Shaanxi	38.14	109.42	79–95	9.7 (0.5)	324 (86)	169 (68)
Xi'an	Shaanxi	34.25	108.90	59–87	14.4 (0.4)	546 (118)	275 (58)
Nanjing	Jiangsu	32.00	118.80	59–89	15.9 (0.5)	1016 (198)	487 (102)
Suzhou	Jiangsu	31.16	120.37	79–95	16.0 (0.8)	971 (387)	504 (164)
Xuzhou	Jiangsu	34.32	117.37	51–80	14.6 (0.5)	869 (200)	307 (111)
Chengdu	Sichuan	30.67	104.07	58–77	16.7 (0.3)	977 (210)	185 (56)

[a] Latitude north and longitude east in degrees and decimals.
[b] Length of daily climate record.
[c] Growing period is time between simulated sowing and maturity.

growing period precipitation (defined as days between simulated sowing and maturity). The wheat growing period corresponds to the dry period of the year at all sites. In general, this period also shows large interannual variability. At the drier sites (Beijing, Yulin, and Liaocheng), the growing season precipitation is less than 200 mm and its coefficient of variation varies from 21 to 55%, implying risk of dryland crop failures and the need for supplemental irrigation to meet crop water requirements.

Soil. Characteristics of the soil at each site needed as crop model inputs include albedo and runoff curve number. For each soil layer, inputs include depth, texture, water-holding capacity at drained lower and upper limits, and at saturation, bulk density, pH, and organic carbon. These characteristics were specified for the crop model simulations at each site based on Jin et al. ([12] and personal communication), the Chinese Soil Taxonomic Classification System (1991), ISSAS and ISRIC (1995), and Zheng et al. (1994) (table 2). The agricultural soils across the range of sites are representative of the major areas where wheat is grown in China (see figure 1). They are fairly uniform across the sites tested, being primarily sandy and sandy loams of medium depth, with neutral pH and low-to-moderate levels of organic carbon. It is important to note that dynamic process crop growth models such as the one used in this work require layered soil-profile characteristics that are often not specified with adequate detail in currently published global or regional soils databases.

In addition to the site-specific soils, a generic soil was created by selecting the median value of the soil characteristics over all sites (table 2). This was done so that crop model simulations with the generic soil could be compared to simulations with the site-specific soils, providing an initial test of the sensitivity of the results to soil specification.

Management variables. Cultivars, planting dates, and plant population (200 plants/m^2) were specified based on current practices and crop cultivar calibration and validation as described by Jin et al. ([12] and personal communication) (table 3). Nitrogen is assumed to be broadcast as ammonium nitrate before planting (30 kg ha^{-1}), with the remainder applied in the spring. Initial soil ammonium and nitrate concentrations are from the Chinese Academy of Agricultural Sciences. Initial soil water was calculated for each site by running the model for the entire time-series of weather and averaging the soil moisture at planting time. The soil-water component was initiated ten days before sowing date.

2.4. Simulations

Three sets of simulations were done:

(1) *Validation.* The first set of simulations was run with observed soils, cultivars, and management for comparison to observed wheat development stages and yields. Data on output and sown areas of wheat were available by county administrative level (Chinese State Land Administration). These aggregated county-level data on wheat production were compared with province-level production reported by the State Statistical Bureau and were found to be in good agreement. For nitrogen and water applications, county-level data for 1989/1990 from the IIASA-LUC database for total fertilizer applications (divided by the number of crops per year) and irrigated percentage of crop production were aggregated to prefecture level. Observed wheat yield data were also aggregated to the prefecture level and represent average wheat yield for all types of production within the administrative unit.

(2) *Potential yield.* The second set utilized automatic nitrogen and irrigation applications according to the specifications shown in table 4. The results of these simulations provide the yield potential with non-limiting nitrogen and water conditions at each site, given current climate and management conditions. Because system efficiencies are set at 100%, nitrogen and water results for these simulations represent net crop nitrogen demand and net irrigation water demand, not actual amounts applied in the field. These simulations were done both with the site-specific soils and the generic soil.

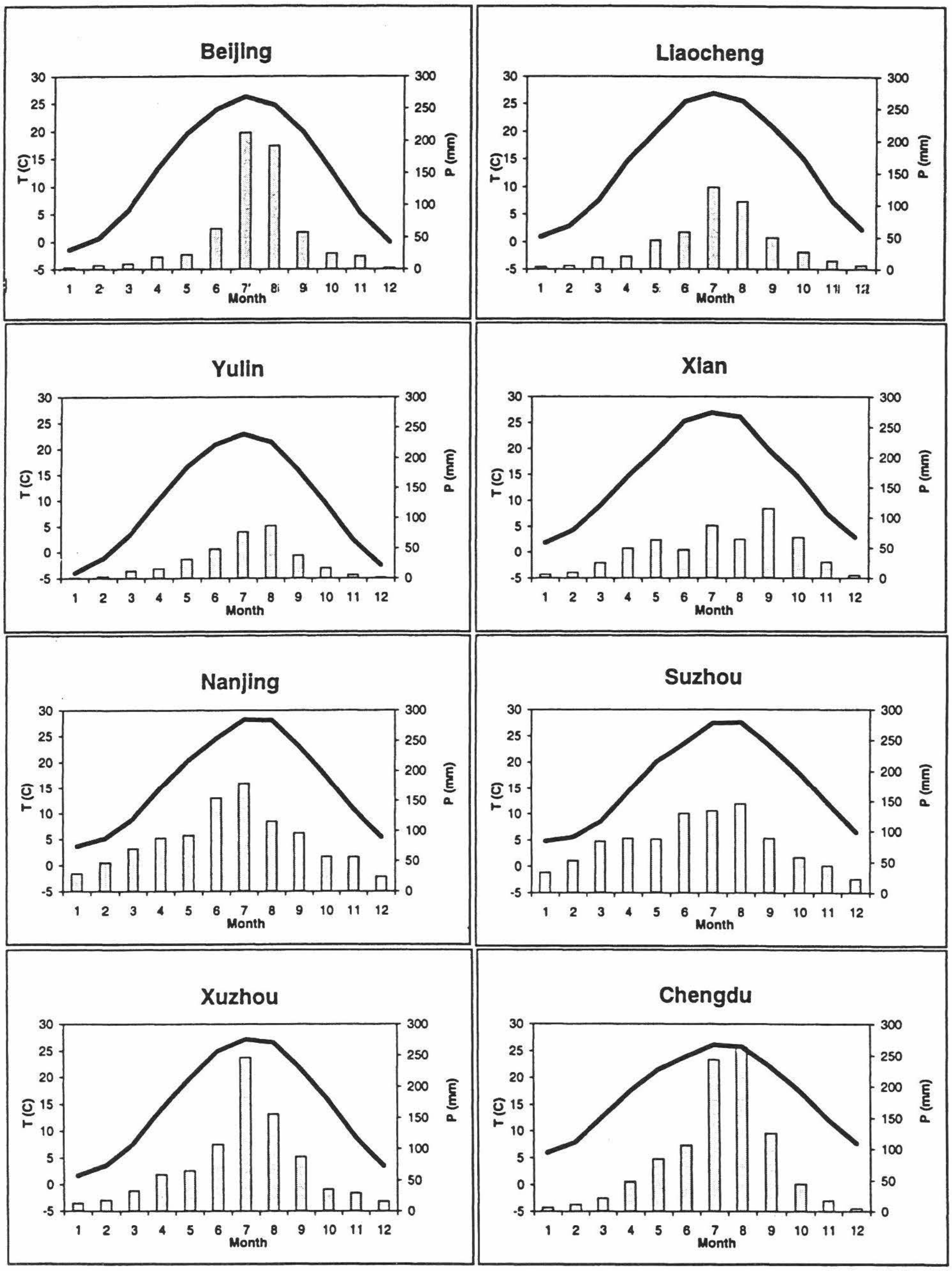

Figure 2. Observed temperature and precipitation at the study sites.

Table 2
Soil inputs for crop model simulations.

Site	CSTCS soil group	Depth (cm)	Texture	Top 30 cm soil layer: Water content: Lower limit (vol%)	Drained upper limit (vol%)	Saturation (vol%)	Bulk density	pH	Organic carbon (%)
Beijing	Cinnamon	87	Sandy	7.1	19.7	47.5	1.25	8.3	1.47
Liaocheng	Yellow brown	124	Sandy-clay	8.3	21.0	42.3	1.32	8.3	0.52
Yulin	Yellow brown	75	Sandy	9.8	21.6	46.5	1.20	8.1	0.52
Xi'an	Heilu soil	115	Sandy	2.1	15.4	44.9	1.25	7.9	0.80
Nanjing	Yellow brown	75	Sandy-loam	9.8	21.6	46.5	1.20	6.5	1.70
Suzhou	Yellow brown	124	Sandy-clay	8.3	21.0	42.3	1.32	6.4	1.80
Xuzhou	Yellow brown	100	Sandy	2.6	12.2	34.6	1.59	8.3	0.53
Chengdu	Purple	110	Silt-loam	16.5	29.6	34.9	1.50	6.5	1.07
All sites	Generic soil	96	Sandy-loam	8.3	20.0	42.7	1.32	7.0	1.50

Sources: Chinese Soil Taxonomic Classification System (CSTCS (1991), in: ISSAS & ISRIC (1995)), Zheng et al. (1994).

Table 3
Planting date, wheat cultivars, and genetic coefficients [12].

Site	Planting date	Cultivar[a]: Name	P1V	P1D	P5	G1	G2	G3
Beijing Liaocheng Yulin	29 September	F.K. 2	4.0	3.8	2.4	3.5	4.3	3.0
Xi'an	10 October	Y.M. 2	6.5	4.2	5.5	5.5	5.5	3.0
Nanjing Suzhou	25 October	Yanmai 5	6.0	4.0	2.0	5.5	5.0	2.0
Xuzhou	10 October	Jinan 13	4.0	4.8	4.0	4.5	4.2	2.0
Chengdu	2 November	M.Y. 11	2.4	4.4	5.0	7.3	4.8	5.0

[a] Genetic coefficients that describe wheat cultivars in the CERES-Wheat model: P1V, vernalization; P1D, photoperiod; P5, grain-filling duration; G1–G3, grain-filling coefficients. The phylochron interval (the thermal time (degree days) between successive leaf tip appearances) coefficient for all cultivars was 95.

Table 4
Automatic management of non-limiting nitrogen and water conditions.

Irrigation	Management depth	50 cm
	Threshold	80% of maximum available water in soil
	End point of applications	100% of maximum available water in soil
	Applications	All growth stages
	Method	Pressure
	Ammount per irrigation	10 mm
	Irrigation efficiency	100%
Nitrogen fertilization	Application depth	15 cm
	Threshold	When crop shows 20% nitrogen stress
	Amount per application	10 kg ha^{-1}
	Material	Ammonium nitrate
	Applications	All growth stages when needed

(3) *Nitrogen–water combinations*. The third set was comprised of combinations of thirteen levels of nitrogen (0, 15, 30, 45, 60, 75, 90, 105, 120, 135, 150, 180, and 210 kg ha^{-1}) and twenty-one levels of irrigation (from 0 to 600 mm in 30 mm increments). For the irrigation treatments, one irrigation treatment was applied before planting; then, after winter dormancy, equal amounts of irrigation were scheduled at varying time intervals, taking into account the specific time-dependent crop water demand at each site (figure 3). Irrigation intervals were longer during the early crop growth stages and shorter in the period from shortly before anthesis up to physiological maturity. This resulted in 4095–8190 simulations per site, depending on length of climate time-series. These simulations were also done with both the site-specific soils and the generic soil.

The CERES-Wheat model outputs analyzed were: dates of anthesis and maturity, grain yield, nitrogen fertilizer applied, and irrigation water amount.

2.5. Statistical analysis and yield functions

Because of the differences in response to nitrogen and irrigation due to climatic differences across the study sites, we calculated temperature and precipitation anomalies for

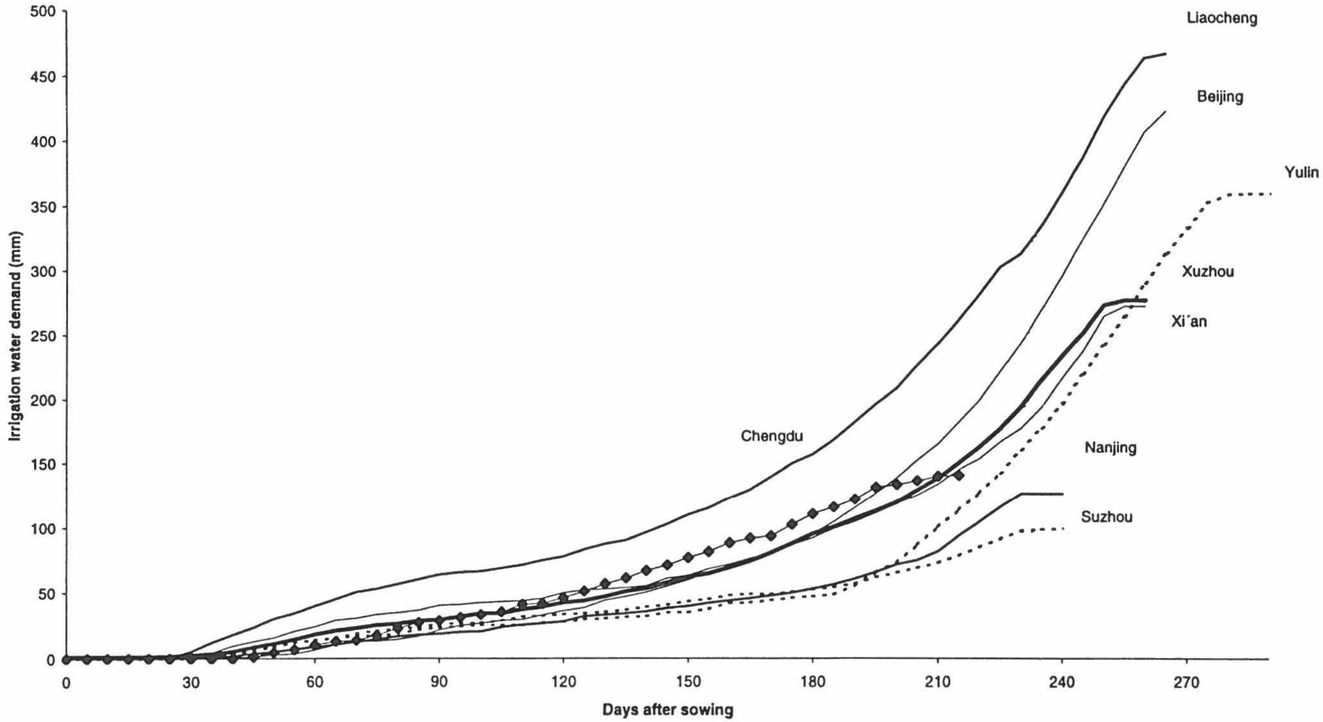

Figure 3. Irrigation water demand with optimal nitrogen fertilization at each site.

March, April, May, and June, and precipitation anomalies over the entire growing period for inclusion in the statistical analysis and yield response functions.

The relationships between wheat yield, input variables, and temperature and precipitation anomalies taken singly were first analyzed using the Pearson product moment correlation coefficient calculated by the SPSS statistical program. This exploratory analysis served to identify variables explaining a significant proportion of the observed yield variance.

Then the quadratic and Mitscherlich–Baule regression models were tested as possible yield functions. For each function, the agreement between the simulated "observed" yields (we now use "observed" to designate the results of the CERES-Wheat simulations) and yields predicted by the functions was measured using the adjusted R^2, representing the fraction of variation in simulated yield explained by the fitted yield values. We also assessed the significance of the estimated models by screening the values obtained for the F-test. F values were less than 0.0001 at the 95% significance level. Function parameters, their significance, and predicted yields were calculated using the SPSS statistical program.

3. Results and discussion

3.1. Comparison of simulated and observed phenology and yields

Table 5 shows a comparison of simulated and observed dates of sowing, anthesis and maturity for wheat at the eight sites. The selected sowing dates and observed phenology were derived from information published by the USDA Foreign Agricultural Service [3]. In general, the crop model simulates anthesis and crop maturity somewhat earlier than observations. The crop model defines anthesis as the date when 50% of the crop is shedding pollen; observations in the field for this stage are often made slightly later. Physiological maturity, simulated as the day that grain-filling ends, is rarely measured in the field; rather, observations of harvest dates may be made two or more weeks later. Since wheat crop nitrogen and water requirements in the latter part of the phenological cycle are usually small, the discrepancy in maturity dates is not likely to affect the use of the model to determine nitrogen and water response functions.

Table 6 shows the fertilizer and irrigation management used in the validation simulations and comparisons

Table 5
Observed and simulated dates of sowing, anthesis and maturity for wheat.

Site	Planting date		Anthesis date		Maturity date	
	Selected for simulations	Observed	Simulated	Observed	Simulated	Observed
Beijing	29 Sept	15 Sept–15 Oct	23 May	15 May–15 Jun	22 Jun	1–15 July
Liaocheng	29 Sept	15 Sept–15 Oct	16 May	15 May–15 Jun	15 Jun	1–15 July
Yulin	29 Sept	15 Sept–15 Oct	2 Jun	15 May–15 Jun	4 July	1–15 July
Xi'an	10 Oct	15 Sept–15 Oct	18 May	15 May–15 Jun	19 Jun	15–30 Jun
Nanjing	25 Oct	1–31 Oct	14 May	15 May–15 Jun	12 Jun	15–30 Jun
Suzhou	25 Oct	1–31 Oct	15 May	15 May–15 Jun	13 Jun	1–15 Jun
Xuzhou	10 Oct	15 Sept–15 Oct	20 May	15 May–15 Jun	18 Jun	15–30 Jun
Chengdu	2 Nov	15 Oct–15 Nov	22 Apr	1–30 Apr	26 May	1–15 Jun

Source of observations: [3]. Source of simulations: average of 15 years with the management described in tables 2 and 3.

Table 6
Yield validation simulations and observations.

Site	No. of counties	Observations[a]			Simulations[b]		
		Total fertilizer/ sown ha (kg ha^{-1})	Share of irrigation (%)	Wheat yield (kg ha^{-1})	Nitrogen fertilizer (kg ha^{-1})	Wheat irrigation (%)	Wheat yield (kg ha^{-1})
Beijing	9	227 (38)[c]	81 (1)	4,518 (43)	150 (0)	80 (0)	4,715 (326)
Liaocheng	8	216 (27)	85 (5)	4,546 (388)	150 (0)	80 (0)	4,926 (664)
Yulin	12	27 (29)	12 (13)	454 (370)	30 (0)	10 (0)	578 (649)
Xi'an	7	180 (58)	70 (23)	2,955 (742)	100 (0)	50 (0)	3,533 (534)
Nanjing	6	183 (36)	94 (5)	2,416 (807)	50 (0)	50 (0)	5,511 (560)
Suzhou	7	262 (73)	99 (1)	2,940 (1,853)	75 (0)	50 (0)	3,783 (786)
Xuzhou	7	276 (55)	72 (15)	3,549 (399)	100 (0)	50 (0)	4,108 (975)
Chengdu	13	127 (29)	85 (12)	3,852 (1,410)	75 (0)	50 (0)	4,251 (493)

[a] For nitrogen and water applications, county-level data for 1989/1990 from the IIASA-LUC database for total fertilizer applications (divided by the number of crops per year) and irrigated percentage of cultivated land were aggregated to prefecture level. Observed wheat yield data were also aggregated to the prefecture level and represent average wheat yields for all types of production within the administrative unit.

[b] The simulations are the average of the period specified in table 1 for each site with management shown in tables 2 and 3. Nitrogen and irrigation simulation inputs were derived from observed values, adjusted for wheat by the characteristics of the cropping system at each site.

[c] Average (standard deviation).

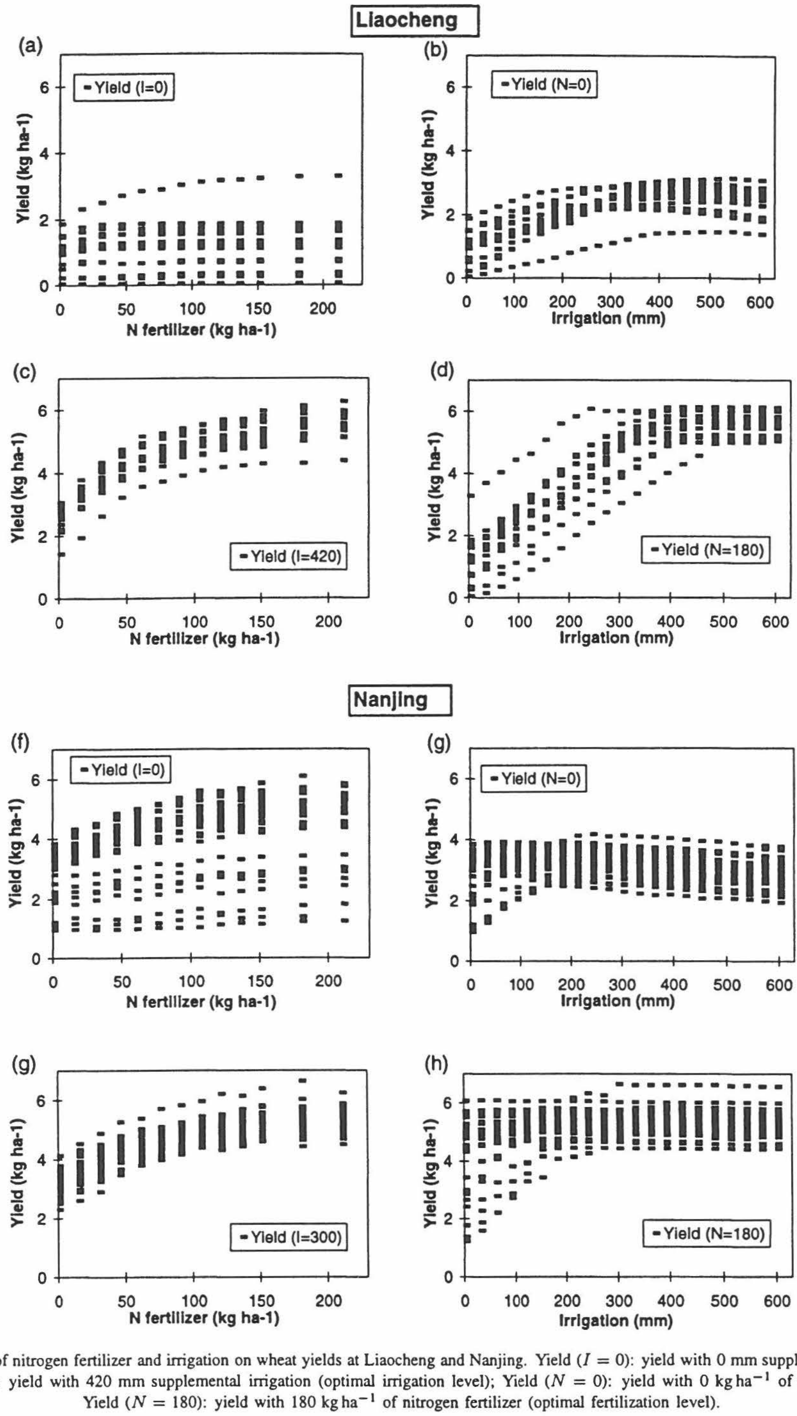

Figure 4. Effect of nitrogen fertilizer and irrigation on wheat yields at Liaocheng and Nanjing. Yield ($I = 0$): yield with 0 mm supplemental irrigation; Yield ($I = 420$): yield with 420 mm supplemental irrigation (optimal irrigation level); Yield ($N = 0$): yield with 0 $\mathrm{kg\,ha^{-1}}$ of nitrogen fertilizer; Yield ($N = 180$): yield with 180 $\mathrm{kg\,ha^{-1}}$ of nitrogen fertilizer (optimal fertilization level).

Table 7
Simulated wheat yield, nitrogen fertilizer applied and irrigation amount.

Site	Site soil			Generic soil		
	Yield ($kg\ ha^{-1}$)	Nitrogen ($kg\ ha^{-1}$)	Irrigation (mm)	Yield ($kg\ ha^{-1}$)	Nitrogen ($kg\ ha^{-1}$)	Irrigation (mm)
Beijing	4,531 (329)	74 (10)	463 (69)	4,412 (428)	91 (57)	427 (72)
Liaocheng	5,216 (405)	141 (48)	443 (56)	5,190 (463)	123 (21)	426 (81)
Yulin	5,237 (256)	67 (10)	402 (38)	4,978 (284)	70 (10)	358 (39)
Xi'an	5,158 (431)	92 (15)	277 (58)	5,077 (457)	108 (18)	271 (57)
Nanjing	4,972 (406)	100 (11)	153 (64)	4,852 (455)	109 (15)	125 (56)
Suzhou	5,457 (678)	137 (22)	89 (61)	5,415 (737)	136 (23)	98 (67)
Xuzhou	4,801 (531)	112 (21)	311 (71)	4,764 (522)	94 (17)	276 (75)
Chengdu	5,240 (373)	57 (7)	136 (40)	5,463 (435)	74 (15)	139 (40)

Table 8
Correlation coefficients between wheat yields and management inputs (nitrogen fertilizer and irrigation amounts) and observed climate anomalies (temperature and precipitation) (a, b). Correlation coefficients between observed monthly temperature and precipitation (c).

Factor	Correlation coefficients							
	Beijing	Liaocheng	Yulin	Xi'an	Nanjing	Suzhou	Xuzhou	Chengdu
(a) Input (nitrogen and water) limited yield								
Nitrogen	0.08	0.10	0.15	0.32	0.56	0.42	0.17	0.26
Irrigation water	0.73	0.71	0.60	0.39	−0.05	−0.02	0.44	0.18
PA3	0.36	0.50	0.12	−0.02	0.20	0.52	−0.03	0.49
PA4	0.51	−0.02	0.29	0.25	0.39	0.47	0.45	0.56
PA5	0.74	0.64	0.39	0.64	0.34	0.69	0.61	0.21
PA6	0.12	0.16	0.39	0.25	0.28	0.33	−0.15	0.31
PAGP	0.44	0.48	0.59	0.37	0.38	0.78	0.64	0.75
TA3	−0.24	0.11	−0.23	−0.07	−0.09	0.53	0.16	−0.20
TA4	−0.01	−0.30	0.11	0.16	−0.02	0.53	0.14	−0.12
TA5	0.03	−0.31	−0.33	−0.47	−0.42	−0.29	−0.60	−0.54
TA6	−0.06	0.06	−0.41	−0.52	−0.20	−0.07	−0.51	–
(b) Water non-limited yield								
Nitrogen	0.86	0.86	0.90	0.84	0.86	0.79	0.79	0.76
TA3	0.03	−0.10	−0.08	0.08	0.08	0.22	0.06	0.01
TA4	0.18	−0.15	0.07	0.07	0.07	0.32	0.16	0.08
TA5	−0.22	−0.25	0.05	−0.04	−0.11	−0.28	−0.24	−0.23
TA6	−0.13	−0.06	−0.20	0.05	0.08	0.07	−0.08	–
(c) Observed weather								
January	0.04	−0.39	−0.70	−0.45	−0.05	0.13	−0.04	−0.33
February	0.27	0.26	0.39	0.15	−0.02	0.27	−0.14	−0.52
March	−0.14	−0.03	0.50	0.03	0.07	0.10	0.10	−0.19
April	−0.31	−0.31	0.32	−0.41	0.16	0.23	0.11	0.26
May	−0.18	−0.29	−0.04	−0.44	−0.35	−0.18	−0.39	0.17
June	−0.34	−0.09	−0.32	−0.61	0.06	−0.09	0.05	0.16
July	−0.18	−0.04	−0.23	−0.75	−0.51	0.06	−0.30	0.12
August	−0.09	0.25	−0.36	−0.59	−0.48	−0.64	−0.41	−0.27
September	−0.10	−0.25	−0.43	−0.47	0.03	0.45	0.18	0.16
October	−0.06	−0.11	0.17	−0.39	−0.05	−0.13	−0.08	0.27
November	0.27	−0.02	−0.20	−0.20	0.08	−0.22	−0.04	0.24
December	0.26	0.35	−0.01	−0.38	0.36	−0.16	0.11	−0.03

PA3-6 = precipitation anomaly of calendar months 3–6; PAGP = precipitation anomaly during the entire growing period; TA3-6 = temperature anomaly of calendar months 3–6.

of observed and simulated wheat yields. Reported fertilizer applications and percent of crop production that is irrigated for the prefecture in which the sites are located are used to derive the input values used in the CERES-Wheat simulations. The high reported fertilizer applications at some sites were reduced to take account of multiple crops per year. Similarly, since the high reported irrigation percentage in Xi'an, Nanjing, Suzhou, Xuzhou, and Chengdu reflects the use of irrigation for all crops (especially rice), we set the irrigation percentage for the validation simulations for these sites at 50%.

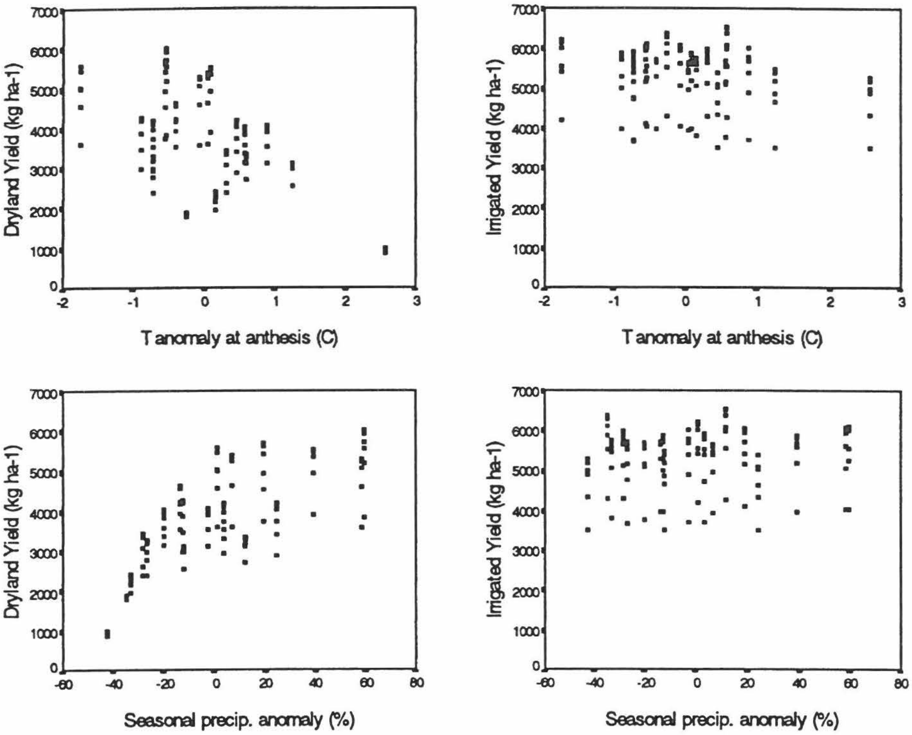

Figure 5. Effects of variation in the observed temperature during the anthesis period (month 5) and growing precipitation on simulated dryland and fully irrigated wheat yields at Chengdu.

Table 9
Simulated wheat yield response to nitrogen and irrigation in Liaocheng.

N fertilizer	Irrigation (mm)										
(kg ha^{-1})	0	60	120	180	240	300	360	420	480	540	600
0	930	1287	1627	1913	2170	2364	2481	2514	2502	2462	2374
15	1067	1516	1946	2325	2671	2929	3116	3181	3181	3162	3085
30	1126	1643	2145	2604	3045	3388	3612	3715	3746	3729	3682
45	1150	1725	2299	2807	3313	3742	4015	4163	4199	4184	4137
60	1172	1774	2385	2970	3510	3998	4339	4485	4549	4530	4509
75	1179	1814	2459	3072	3631	4192	4500	4703	4764	4749	4730
90	1199	1837	2508	3155	3731	4311	4674	4866	4951	4933	4929
105	1202	1869	2544	3219	3830	4440	4810	5001	5065	5057	5047
120	1209	1865	2579	3259	3908	4514	4891	5087	5161	5176	5149
135	1213	1882	2615	3320	3972	4604	4967	5141	5247	5245	5240
150	1220	1894	2643	3352	4011	4655	5095	5277	5361	5373	5365
180	1235	1907	2615	3399	4099	4789	5217	5395	5472	5477	5485
210	1238	1904	2635	3426	4148	4840	5270	5476	5551	5547	5566

Simulated yields are generally higher than observed, but represent reported yields fairly well. The model simulates the yield of fully irrigated wheat better than that of less well-watered wheat, since water stress, a major source of yield variation, is eliminated in those circumstances. Finally, the models do not consider limitations due to nutrients other than nitrogen, nor possible yield reductions caused by weeds, pests and diseases, and flooding; thus crop model simulations are usually taken to represent an upper limit of crop production for the management systems and sites tested.

3.2. Potential yield

Table 7 shows modeled wheat yields, nitrogen applications, and irrigation amount under non-limiting nitrogen

Quadratic 1: $Yi = \alpha_1+\alpha_2(Ni)+\alpha_3(Ii)+\alpha_4(Ni)^2+\alpha_5(Ii)^2+\alpha_6(N_iI_i)$

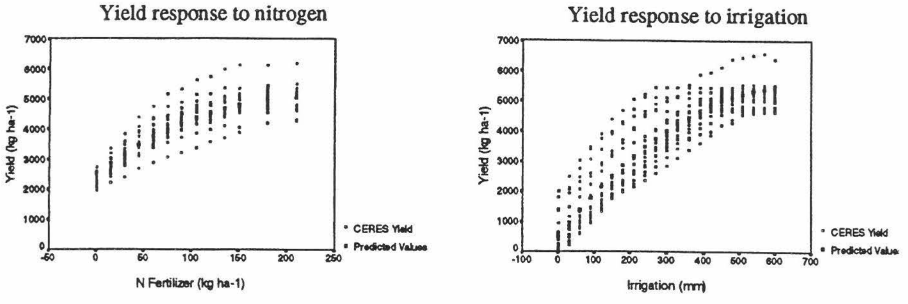

Quadratic 2: $Yi = \alpha_1+\alpha_2(Ni)+\alpha_3(Ii+Pi)+\alpha_4(Ni)^2+\alpha_5(Ii+Pi)^2+\alpha_6(N_i(Ii+Pi))$

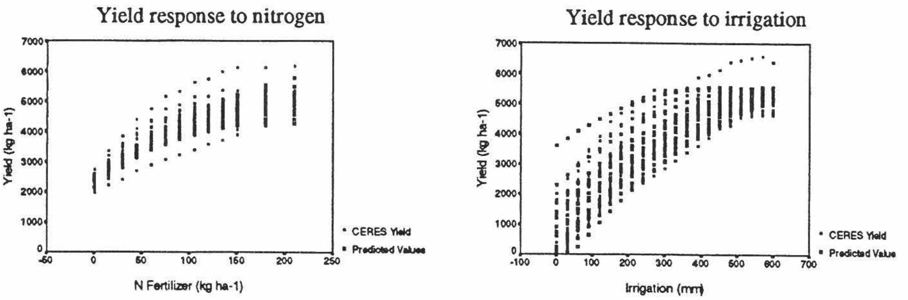

Figure 6. CERES-Wheat and predicted yields with quadratic non-linear regression models at Beijing.

and water regimes. Potential yields give an indication of the maximum yield possible under current climate and management conditions and are fairly similar across the transect of sites. High N applications are related to low initial fertility levels of the sites (Liaocheng and Suzhou), and water applications are highest in the dry sites (Beijing, Yulin, and Liaocheng). The large difference between potential and validated yield at Yulin demonstrates the ability of intensive management to overcome water- and nitrogen-limited conditions.

Differences between the site-specific soils and the generic soil have minor effects on potential yield, simulated nitrogen fertilizer applied, and irrigation amount. This is likely to be the case because agricultural soils in the study region of China as described by the LUC database have similar low water-holding capacities and nitrogen-supplying abilities. The effect on yields of using a generic soil rather than a site-specific soil was within 5%.

3.3. Nitrogen–water combinations

Figure 4 shows the effect of nitrogen fertilizer and irrigation on simulated wheat yields at Liaocheng, a dry site, and Nanjing, a well-watered site. The points represent the simulated yield values for each year. At both wet and dry sites, the variation of yield for a particular nitrogen level is smaller if the crop is well-watered and larger in dryland settings. Across nitrogen levels, more benefit is found to fertilizer application in irrigated rather than dryland crops, since nutrient uptake is limited under dry conditions. The dry site displays lower response to nitrogen and lower yields; the greatest response is seen at the dry site when irrigation is applied at high nitrogen fertilization.

Crop responses at Beijing and Yulin are similar to the one at Liaocheng; those at Chengdu and Suzhou are similar to that of Nanjing; responses at Xi'an and Xuzhou are intermediate. At Chengdu, the response to nitrogen fertilizer is very similar in dryland and irrigated simulations because of the high precipitation regime.

3.4. Statistical analysis and yield functions

Correlation coefficients. Table 8(a) shows the correlation coefficients at the eight sites between wheat yields, inputs (nitrogen and water) and variations in temperature and precipitation in the observed climate record. Climate anomalies are for March to June when the crop is actively growing. As expected, yields at drier sites are less well-correlated with nitrogen fertilizer applications than yields at wetter sites; yields at drier sites are, of course, highly cor-

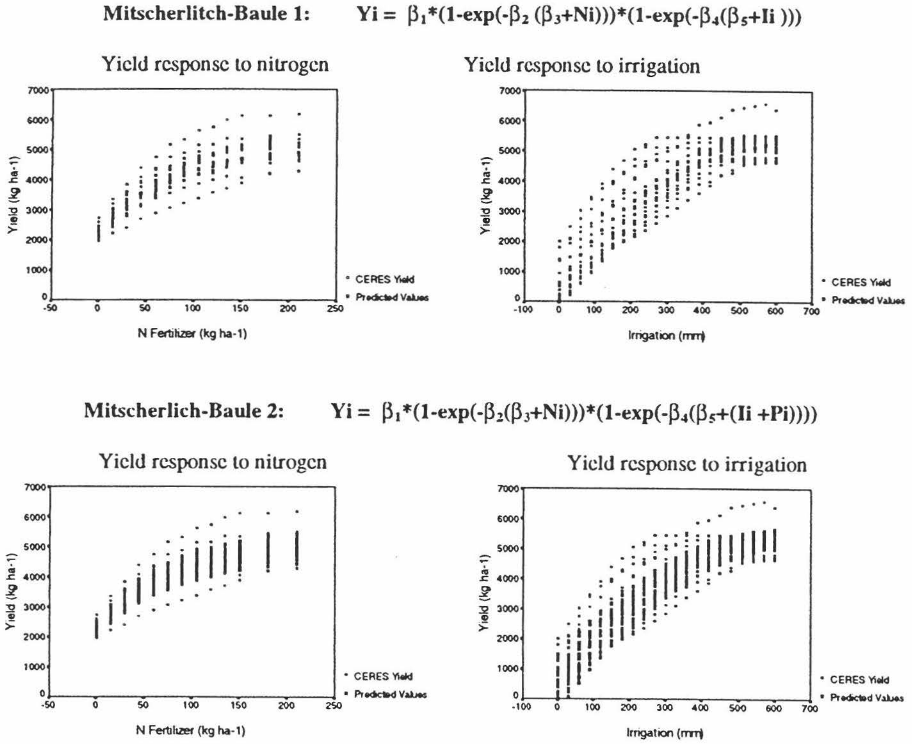

Figure 7. CERES-Wheat and predicted yields with Mitscherlich-Baule models at Beijing.

Table 10

Adjusted R^2 values of the predicted yields with the Quadratic 2 and Mitscherlich–Baule 2 regression models.

Site	Site soil		Generic soil	
	Quadratic	Mitscherlich–Baule	Quadratic	Mitscherlich–Baule
Beijing	0.838	0.839	0.834	0.835
Liaocheng	0.810	0.812	0.805	0.870
Yulin	0.858	0.856	0.867	0.862
Xi'an	0.659	0.668	0.719	0.724
Nanjing	0.564	0.560	0.741	0.728
Suzhou	0.599	0.590	0.539	0.533
Xuzhou	0.544	0.543	0.486	0.496
Chengdu	0.598	0.657	0.623	0.689

Quadratic 2: $Y_i = \alpha_1 + \alpha_2(N_i) + \alpha_3(I_i + P_i) + \alpha_4(N_i)^2 + \alpha_5(I_i + P_i)^2 + \alpha_6(N_i(I_i + P_i))$.
Mitscherlich–Baule 2: $Y_i = \beta_1(1 - \exp(-\beta_2(\beta_3 + N_i)))(1 - \exp(-\beta_4(\beta_5 + (I_i + P_i))))$.
All values are significant at the 95% level.

related with irrigation amounts. Yields at the different sites respond differently to precipitation anomalies in the individual months of the growing period, due to differences in crop–climate interactions. In general, however, yields are positively correlated with precipitation anomalies in May and over the growing period.

Yields are negatively correlated with temperature anomalies from March to June, especially in May and June at Yulin, Xi'an, Nanjing, Xuzhou, and Chengdu. However, temperature–yield correlations in general are lower than precipitation–yield correlations. Temperature effects are important at warmer sites where high temperatures limit an already short duration of grain-filling.

Table 8(b) shows correlations of non water-limited yields with nitrogen fertilizer applications and temperature anomalies in March, April, May, and June. Non-water-limited

Table 11
Estimated coefficients in the Quadratic 2 and Mitscherlich-Baule 2 models.

Site	Quadratic			Mitscherlich-Baule		
	Parameter	Site soil	Generic soil	Parameter	Site soil	Generic soil
Beijing	α_1	101.805	64.810	β_1	6409.010	6266.932
		(5.6)	(4.3)		(154.8)	(165.4)
	α_2	10.504	12.201	β_2	0.013	0.013
		(34.0)	(36.5)		(56.2)	(65.4)
	α_3	11.146	10.723	β_3	55.569	45.610
		(35.2)	(26.8)		(24.6)	(32.7)
	α_4	−0.047	−0.054	β_4	0.003	0.004
		(26.7)	(26.2)		(46.5)	(56.2)
	α_5	−0.011	−0.012	β_5	24.900	25.470
		(22.4)	(21.0)		(36.7)	(36.3)
	α_6	0.021	0.025			
		(4.5)	(3.2)			
Liaocheng	α_1	380.117	396.532	β_1	6259.596	6528.261
		(4.2)	(3.6)		(143.8)	(136.5)
	α_2	15.460	14.211	β_2	0.018	0.018
		(42.0)	(41.2)		(67.0)	(74.2)
	α_3	11.792	10.633	β_3	37.08	36.858
		(44.1)	(39.6)		(21.4)	(26.3)
	α_4	−0.066	−0.064	β_4	0.004	0.003
		(31.2)	(27.9)		(46.9)	(42.7)
	α_5	−0.013	−0.011	β_5	47.652	52.059
		(26.1)	(27.0)		(34.1)	(37.2)
	α_6	0.023	0.025			
		(5.6)	(5.6)			
Yulin	α_1	251.521	225.207	β_1	6829.595	6671.819
		(8.9)	(7.8)		(158.2)	(192.4)
	α_2	14.880	19.874	β_2	0.015	0.014
		(48.9)	(47.2)		(75.2)	(73.4)
	α_3	14.596	14.685	β_3	47.317	36.491
		(45.0)	(38.1)		(46.7)	(46.2)
	α_4	−0.066	−0.084	β_4	0.004	0.006
		(25.3)	(19.8)		(46.4)	(56.2)
	α_5	−0.017	−0.019	β_5	27.354	27.182
		(17.6)	(19.0)		(36.5)	(42.3)
	α_6	0.026	0.031			
		(6.4)	(5.7)			
Xi'an	α_1	1972.621	1450.836	β_1	5863.469	5896.637
		(6.8)	(4.3)		(134.6)	(143.2)
	α_2	17.632	21.962	β_2	0.014	0.014
		(34.6)	(37.2)		(45.6)	(49.1)
	α_3	10.025	9.543	β_3	63.950	45.825
		(42.1)	(42.0)		(26.2)	(27.9)
	α_4	−0.059	−0.074	β_4	0.010	0.009
		(24.9)	(22.6)		(14.7)	(12.5)
	α_5	−0.014	−0.014	β_5	72.601	69.597
		(18.2)	(17.0)		(27.3)	(24.2)
	α_6	0.011	0.017			
		(7.6)	(4.2)			
Nanjing	α_1	2989.912	2698.605	β_1	5480.658	5473.280
		(4.3)	(3.5)		(113.2)	(119.2)
	α_2	19.090	26.388	β_2	0.013	0.013
		(32.2)	(34.1)		(45.7)	(52.1)
	α_3	2.754	0.781	β_3	66.621	43.477
		(16.3)	(12.9)		(22.6)	(19.6)
	α_4	−0.059	−0.080	β_4	0.016	0.032
		(19.2)	(19.6)		(32.5)	(37.8)
	α_5	−0.005	−0.003	β_5	110.087	79.695
		(8.9)	(10.2)		(23.6)	(26.6)
	α_6	0.008	0.010			
		(3.2)	(3.5)			

Table 11
(Continued.)

Site	Quadratic			Mitscherlich–Baule		
	Parameter	Site soil	Generic soil	Parameter	Site soil	Generic soil
Suzhou	α_1	3096.824	2921.747	β_1	5912.683	5919.427
		(3.6)	(2.7)		(137.4)	(135.1)
	α_2	26.107	26.016	β_2	0.013	0.013
		(34.4)	(36.3)		(56.7)	(62.0)
	α_3	0.407	1.186	β_3	48.799	48.825
		(19.5)	(20.7)		(22.6)	(29.2)
	α_4	−0.077	−0.076	β_4	0.045	0.027
		(20.1)	(21.4)		(19.5)	(16.5)
	α_5	−0.003	−0.004	β_5	63.229	86.139
		(11.2)	(9.6)		(13.2)	(9.6)
	α_6	0.010	0.010			
		(3.4)	(2.6)			
Xuzhou	α_1	1137.251	1568.308	β_1	5275.731	5390.450
		(6.9)	(4.3)		(144.2)	(165.3)
	α_2	19.859	17.203	β_2	0.013	0.015
		(34.5)	(29.3)		(62.6)	(66.3)
	α_3	6.934	8.852	β_3	38.330	54.793
		(16.3)	(14.0)		(21.0)	(34.2)
	α_4	−0.070	−0.058	β_4	0.007	0.008
		(32.9)	(34.2)		(22.6)	(21.9)
	α_5	−0.010	−0.011	β_5	87.214	81.861
		(12.1)	(10.0)		(12.7)	(11.5)
	α_6	0.020	0.011			
		(3.1)	(2.8)			
Chengdu	α_1	3549.224	3234.610	β_1	5801.356	5789.534
		(3.2)	(2.8)		(126.4)	(134.1)
	α_2	22.602	24.760	β_2	0.025	0.025
		(36.2)	(38.1)		(48.9)	(44.2)
	α_3	4.420	5.006	β_3	43.686	39.562
		(12.0)	(10.6)		(25.1)	(22.0)
	α_4	−0.083	−0.092	β_4	0.030	0.026
		(38.9)	(42.0)		(16.1)	(15.6)
	α_5	−0.008	−0.008	β_5	45.934	47.277
		(6.5)	(4.2)		(15.4)	(12.3)
	α_6	0.007	0.008			
		(2.1)	(2.0)			

Note: Statistics in parentheses are t statistics, all significant at the 1% level.

wheat yields are highly correlated with nitrogen fertilizer levels at all sites. As with the yields in the nitrogen–water combinations, the effects of temperature anomalies during March through April on yields in the non-limiting water simulations are generally small.

From this analysis, it appears that nitrogen fertilization level, irrigation amount, and precipitation anomalies are important variables to include in the functional forms for these sites. Temperature, while displaying lower correlation with yield at the study sites, is also important in explaining yield variation. However, since variation in temperature was quite low within sites, and since temperature is often (negatively) correlated with precipitation (table 8(c)), temperature was not included in the initial regression model.

An example of the relationships of simulated wheat yield to temperature and precipitation anomalies is shown in figure 5. Dryland yields at Chengdu, a warm site, are negatively correlated to temperature at anthesis over the range of observed anomalies; they are also negatively correlated to decreases in growing season precipitation. In contrast, irrigated yields at Chengdu are correlated to neither of these observed anomalies.

Yield response functions. An example of the yield data from the crop model simulations is shown in table 9 for Liaocheng; each value is the average of crop model simulations for the years of climate record (in this case, 16 years of climate record). At higher input levels (nitrogen applied greater than 120 kg ha^{-1} and irrigation more than 400 mm), a yield plateau of approximately 5500 kg ha^{-1} was reached, representing the biophysical crop yield limit given the specified management conditions. Similar data for each site were used to test the quadratic and MB functional forms.

The functional forms were tested with the inclusion of management inputs (nitrogen fertilizer and irrigation water amounts); then functions including temperature and/or pre-

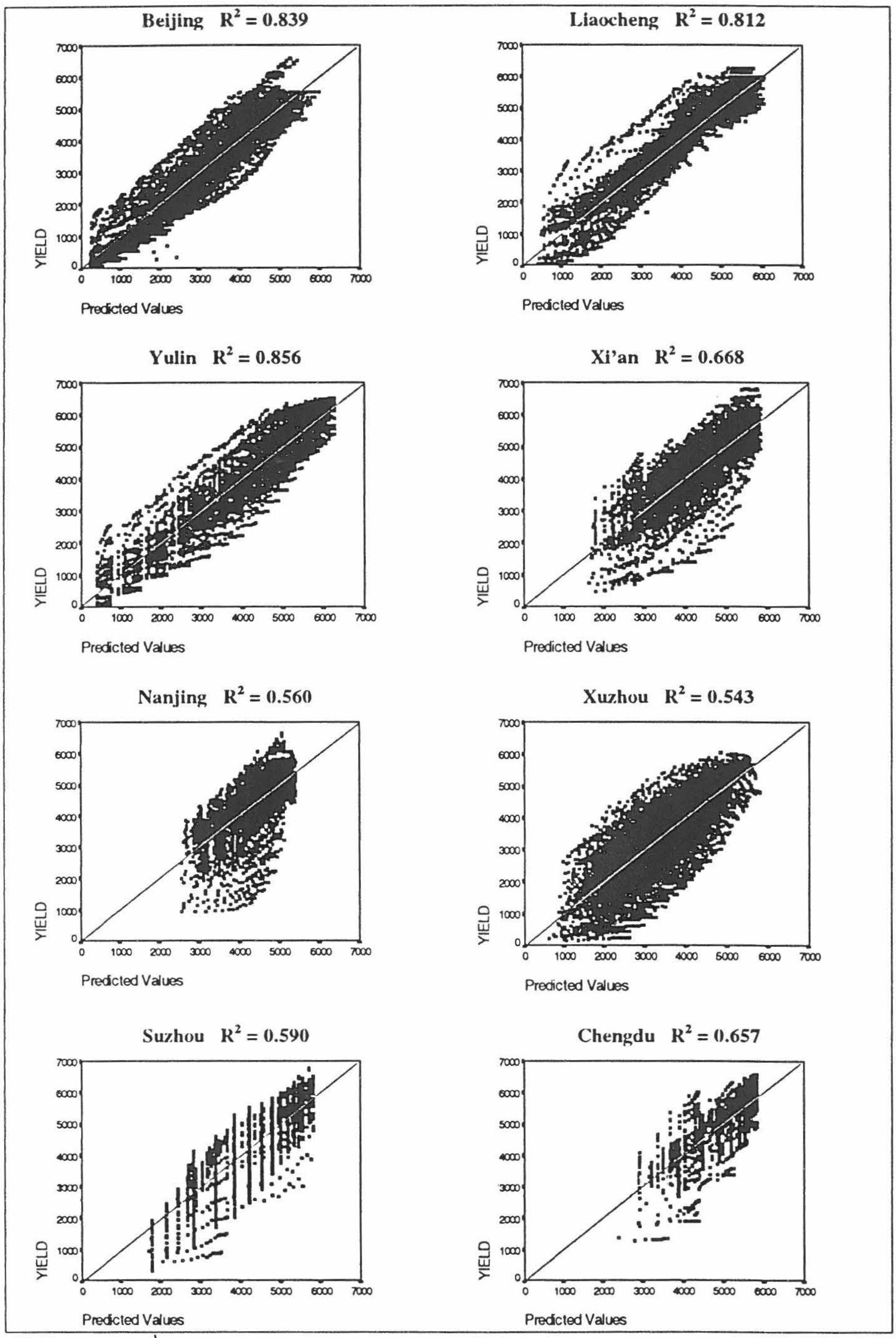

Values on kg ha^{-1}.

Figure 8. Comparison of yields simulated with the CERES-Wheat model and predicted with the Mitscherlich-Baule 2 model.

cipitation anomalies during the growing season were tested. Precipitation anomalies were added to the irrigation water term, providing a term representing the overall water status of the crop during the growing season. The incorporation of temperature anomalies in the functions did not improve the adjustment between observed and predicted yields, and the function parameters in the temperature terms were not significant. This result is likely influenced by the relatively low range of temperature variation and the correlations between temperature and precipitation evident at most sites.

Figures 6 and 7 show CERES-Wheat simulated yields and predicted yields with different specifications of quadratic and MB functions at Beijing. Quadratic 1 and Mitscherlich–Baule 1 (MB1) are the functions with management inputs alone; Quadratic 2 and Mitscherlich–Baule 2 (MB2) include precipitation anomalies. The inclusion of precipitation anomalies in the water term allows for calculation of the effects of year-to-year variation in climate, a useful attribute that allows for consideration of risk in the economic model. Table 10 shows that the adjusted R^2 values obtained with the Quadratic 2 and the MB2 forms are similar, with the R^2 values obtained with MB2 being on average slightly higher. Table 11 shows the parameters in the functional forms (all significant at the 95% level); the MB parameters are more stable than those of the quadratic function. The β_1 parameter represents yield levels that would occur with unconstrained availability of inputs at zero price; this is a hypothetical value, in most cases, higher than the agronomic potential yield shown in table 7. Figure 8 shows a comparison of observed and predicted yields for the site-specific soils with the MB2 function that includes the precipitation variation.

When using the Mitscherlich–Baule function in the context of an optimizing economic model, it is important to note that specifications with more than one input factor (e.g., nutrients and water) exhibit increasing returns to scale [13]. Keyzer [13] has developed a generalized MB function that provides for an even more flexible specification that can be used to control returns-to-scale in estimating agricultural production relations. The more flexible specification of the Mitscherlich–Baule function is

$$Y_i = \beta_1\left(1 - \exp\left(-\beta_2(\beta_3 + N_i)\right)\right)^{\theta_1} \times \left(1 - \exp\left(-\beta_4(\beta_5 + W_i)\right)\right)^{\theta_2}.$$

The adjusted R^2 values are not very sensitive to the use of the generic soil with median characteristics across the main wheat region of China (tables 10 and 11). Thus, the functions may be considered representative of agriculturally productive regions in China under intensifying management conditions. Variation in soil characteristics is more important at lower levels of nitrogen and water inputs than at higher levels.

4. Conclusions

This work links biophysical and economic models in a rigorous and testable methodology. The validated crop model is useful for simulating the range of conditions under which wheat is grown in China, and provides the means to estimate production functions when experimental field data are not available. The Mitscherlich–Baule functional form is preferable to the quadratic form for incorporation into a land-use change model due to its simulation of the growth plateau and input substitutability. Its role in the IIASA LUC model involves both the determination of input demand and output scale, and, through response functions for other crops besides wheat, the determination of product mix.

Further work will involve pooling the data across sites and developing scaling techniques to utilize the estimated functions for wheat throughout the current agricultural region of China. With climate change, the zones where wheat may be grown will likely shift to the North, but the climatic conditions (i.e., a monsoon climate with a dry and cool winter) under which wheat can be grown may be nearly the same. Soils may differ however. Therefore, the crop models will be used to expand the range of the functions' applicability in regard to higher temperature, changed hydrological regimes, wider variation in soil characteristics, higher levels of atmospheric carbon dioxide, and sulfate aerosols, and thus allow for the use of the work for global environmental change projections.

References

[1] C. Ackello-Ogutu, Q. Paris and W.A. Williams, Testing a von Liebig crop response function against polynomial specifications, American Journal of Agricultural Economics 67 (1985) 873–880.

[2] W. Baier, Crop-weather analysis model: Review and model development, Journal of Applied Meterorology 12 (1973) 937–947.

[3] FAS, Foreign Agricultural Service of the U.S. Department of Agriculture (1997).

[4] G. Fischer, Y. Ermoliev, M.A. Keyzer and C. Rosenzweig, Simulating the socio-economic and biogeophysical driving forces of land-use and land-cover change: The IIASA land-use change model, IIASA Working Paper WP-96-010 (1996).

[5] G. Fischer and G.K. Heilig, Population momentum and the demand on land and water resources, Philos. Trans. Roy. Soc. London B 352 (1997) 869–889.

[6] Food and Agriculture Organization of the United Nations (1999); http://apps.fao.org.

[7] M.D. Frank, B.R. Beattie and M.F. Embleton, A comparison of alternative crop response models, American Journal of Agricultural Economics 72 (1990) 597–602.

[8] D.C. Godwin and C.A. Jones, Nitrogen dynamics in soil-plant systems, in: *Modeling Plant and Soil Systems*, Agronomy Series No. 31, eds. J. Hanks and J.T. Ritchie (American Society of Agronomy, Madison, WI, 1991) pp. 287–321.

[9] D. Godwin, J. Ritchie, U. Singh and L. Hunt, *A Users Guide to CERES Wheat, Version 2.10* (International Fertilizer Development Center, Muscle Shoals, AL, 1990) p. 94.

[10] S.S. Grimm, Q. Paris and W.A. Williams, A von Liebig model for water and nitrogen crop response, Western Journal of Agricultural Economics 12 (1987) 182–192.

[11] IIASA, Iiasa.ac.at/Research/LUC/GIS/giswebpage (18 May 1998).

[12] Z. Jin, D. Ge, H. Chen and J. Fang, Effects of climate change on rice production and strategies for adaptation in southern China, in: *Climate Change and Agriculture: Analysis of Potential International Impacts*, Special Publication No. 59, eds. C. Rosenzweig, L.H. Allen, Jr., L.A. Harper, S.E. Hollinger and J.W. Jones (American Society of Agronomy, Madison, WI, 1995) pp. 307–323.

[13] M.A. Keyzer, Formulation and spatial aggregation of agricultural production relationships within the Land Use Change (LUC) model, IR-98-092, International Institute for Applied Systems Analysis, Laxenburg (1998).

[14] G.J. Kovacs, T. Nemeth and J.T. Ritchie, Testing simulation models for the assessment of crop production and nitrate leaching in Hungary, Agricultural Systems 49 (1995) 385–397.

[15] R.V. Llewelyn and A.M. Featherstone, A comparison of crop production functions using simulated data for irrigated corn in western Kansas, Agricultural Systems (1997).

[16] J. Ramirez, C.M. Sakamoto and R.E. Jensen, Wheat, in: *Impacts of Climate Change on the Biosphere*, CIAP Monograph No. 5, Part 2. Climatic Effects (1975) pp. 4-37–4-90.

[17] C.W. Richardson and D.A. Wright, *WGEN: A Model for Generating Daily Weather Variables*, ARS-8 (U.S. Department of Agriculture, Agricultural Research Service, Washington, DC, 1984) p. 83.

[18] J.T. Ritchie, A user-orientated model of the soil water balance in wheat, in: *Wheat Growth and Modelling*, eds. W. Day and R.K. Atkin (Plenum, New York, 1985) pp. 293–306.

[19] J.T. Ritchie, D.C. Godwin and S. Otter-Nacke, *CERES-Wheat. A Simulation Model of Wheat Growth and Development* (Texas A&M University Press, College Station, TX, 1988).

[20] J.T. Ritchie and S. Otter, Description and performance of CERES-Wheat: A user-oriented wheat yield model, in: *ARS Wheat Yield Project*, ARS-38, ed. W.O. Willis (U.S. Department of Agriculture, Agricultural Research Service, Washington, DC, 1985) pp. 159–175.

[21] C. Rosenzweig and D. Hillel, *Climate Change and the Global Harvest: Potential Impacts of the Greenhouse Effect on Agriculture* (Oxford University Press, New York, 1998) p. 336.

[22] C. Rosenzweig and A. Iglesias, The use of crop models for international climate change impact assessment, in: *Understanding Options for Agricultural Production*, eds. G.Y. Tsuji, G. Hoogenboom and P.K. Thornton (Kluwer, Dordrecht, 1998) pp. 267–292.

[23] S.M. Scheierling, G.E. Cardon and R.A. Young, Impact of irrigation timing on simulated water–crop production functions, Irrigation Science 18 (1997) 23–31.

[24] M.A. Semenov, J. Wolf, L.G. Evans, H. Ackersten and A. Iglesias, Comparison of wheat simulation models under climate change, Climate Research 7 (1996) 271–181.

[25] L.M. Thompson, Weather and technology in the production of wheat in the United States, Journal of Soil and Water Conservation 24 (1969) 219–224.

[26] P.E. Waggoner, Agriculture and a climate changed by more carbon dioxide, in: *Changing Climate* (National Academy of Sciences Press, Washington, DC, 1983) pp. 383–418.

[27] J.R. Williams, P.T. Dyke and C.A. Jones, EPIC – A model for assessing the effects of erosion on soil productivity, in: *Proc. 3rd Int. Conf. on State-of-the-Art in Ecological Modelling*, eds. W.K. Lavenroth et al., Fort Collins, CO, 24–28 May 1982 (Elsevier, New York, 1983).

References for China data

Soils

CSTCS, Chinese Soil Taxonomic Classification System (1991), in: *Reference Soil Profiles of the People's Republic of China: Field and Analytical Data* (Institute of Soil Sciences, Academia Sinica, and International Soil Reference and Information Centre, Wageningen, 1995).

Land use

Chinese Academy of Science, Institute of Geography (M. Zhao, personal communication) and Chinese State Land Administration. For details, see G. Fischer, Y. Chen and L. Sun, The balance of cultivated land in China during 1988–1995, Interim Report IR-98-047, International Institute for Applied Systems Analysis, Laxenburg, Austria (1998).

Crops, prices, and county-level data

State Statistical Bureau, *Statistical Yearbook of China, 1989–1997* (China Statistical Publishing House, Beijing, 1989–1997).

State Statistical Bureau, Survey Team of Urban Socio-Economy, *Yearbook of Price Statistics of China, 1992* (China Statistical Publishing House, Beijing, 1992) (in Chinese).

State Statistical Bureau and Center for Development Studies of the State Council, *County Economies of China*, Vols. I–IV (China Statistical Publishing House, Beijing, 1996) (in Chinese).

Crop distribution and production

The crop-specific area and production data for 1987–1989 were prepared within project CPR/87/029, State Land Administration executing agency in China, for FAO. Two relevant reports on crop distribution from this project are:

Z. Zheng, X. Liu, Z. Meng and D. Zheng, *Land Utilization Types in China*, Land Resources, Use and Productivity Assessment in China, Project CPR/87/029, Technical Annex Vol. I, United Nations Development Program, State Science and Technology Commission of the People's Republic of China, Food and Agriculture Organization of the United Nations, State Land Administration of the People's Republic of China (Beijing, 1994) p. 144.

J. Xie and K. Jia, *Potential Assessment of Crop Production*, Land Resources, Use and Productivity Assessment in China, Project CPR/87/029, Technical Annex Vol. III (Beijing, 1994).

The IIASA-LUC GIS webpage: http://www.iiasa.ac.at/Research/LUC/GIS/giswebpage/documents.

Affiliation of Authors

Cynthia Rosenzweig
NASA, Goddard Institute for Space Studies, New York, NY, USA
Ana Iglesias
Polytechnical University of Madrid, Spain
Günther Fischer
International Institute for Applied Systems Analysis, Laxenburg, Austria
Yanhua Liu
The State Commission of Science and Technology, Beijing, China
Walter Baethgen
International Fertilizer Development Center, Montevideo, Uruguay
James W. Jones
University of Florida, Gainesville, FL, USA